

# Subsite mapping of human salivary $\alpha$ -amylase and the mutant Y151M

Lili Kandra<sup>a,\*</sup>, Gyöngyi Gyémánt<sup>a</sup>, Judit Remenyik<sup>b</sup>, Chandran Rangunath<sup>c</sup>,  
Narayanan Ramasubbu<sup>c,\*</sup>

<sup>a</sup> Department of Biochemistry, Faculty of Sciences, University of Debrecen, P.O. Box 55, 4010 Debrecen, Hungary

<sup>b</sup> Research Group for Carbohydrates of the Hungarian Academy of Sciences, P.O. Box 55, 4010 Debrecen, Hungary

<sup>c</sup> Department of Oral Biology, University of Medicine and Dentistry of New Jersey, Newark, NJ 07103, USA

Received 3 March 2003; revised 29 April 2003; accepted 30 April 2003

First published online 13 May 2003

Edited by Stuart Ferguson

**Abstract** This study characterizes the substrate-binding sites of human salivary  $\alpha$ -amylase (HSA) and its Y151M mutant. It describes the first subsite maps, namely, the number of subsites, the position of cleavage sites and apparent subsite energies. The product pattern and cleavage frequencies were determined by high-performance liquid chromatography, utilizing a homologous series of chromophore-substituted maltooligosaccharides of degree of polymerization 3–10 as model substrates. The binding region of HSA is composed of four glycone and three aglycone-binding sites, while that of Tyr151Met is composed of four glycone and two aglycone-binding sites. The subsite maps show that Y151M has strikingly decreased binding energy at subsite (+2), where the mutation has occurred (−2.6 kJ/mol), compared to the binding energy at subsite (+2) of HSA (−12.0 kJ/mol).

© 2003 Federation of European Biochemical Societies. Published by Elsevier Science B.V. All rights reserved.

**Key words:** Human salivary  $\alpha$ -amylase; Y151M mutant; Action pattern; Subsite map; Binding energy; Maltooligosaccharide

## 1. Introduction

$\alpha$ -Amylases (EC 3.2.1.1) catalyze the hydrolysis of  $\alpha$ -1,4 glycosidic linkages in starch and other related carbohydrates. These enzymes are ubiquitous in both the plant and the animal kingdoms and play a key role in carbohydrate metabolism. Human  $\alpha$ -amylases of both salivary (HSA) and pancreatic (HPA) origins have been extensively studied from the viewpoint of clinical chemistry because they are important as indicators in evaluating diseases of pancreas and salivary glands [1,2]. Furthermore, they are used as targets for drug design in attempts to treat diabetes, obesity, hyperlipemia and caries [3]. The overall primary structures of the pancreatic and salivary  $\alpha$ -amylases are highly homologous [4], and high sequence identity between the two enzymes is reflected by a correspondingly high level of structural similarity [3,5].

$\alpha$ -Amylase is the most abundant enzyme in human saliva and consists of two major families with several isoenzyme in each family. Extensive studies referring to the subsite architecture of HSA [6–8] and related enzymes have generated an interest in examining the role of individual residues around the substrate-binding site. The active sites of HSA, HPA and porcine pancreatic  $\alpha$ -amylase (PPA) are very similar in architecture as derived from the crystal structures of the enzyme: acarbose complexes [9,10].

In this study we have invoked the popular ‘subsite model’, which was introduced by Phillips [11], to account for the enzymatic properties of HSA and the mutant Y151M. The amylase subsite model [12] depicts the substrate-binding region of the enzyme to be a tandem array of subsites. Each subsite is complementary to, and interacts with a substrate monomer unit. The subsites are labelled from the catalytic site, with negative numbers for subsites to the left (non-reducing end side) and positive numbers to the right (reducing end side) according to the proposed nomenclature of Davies et al. [13]. There are a number of different ways in which an oligomer substrate can interact with these subsites. A substrate oligomer can bind non-productively so that a susceptible bond does not extend over the catalytic amino acids of the enzyme; alternatively, the substrate can bind productively so that a susceptible bond lies over the catalytic site, in which case the bond is cleaved.

The process of quantifying the subsite model is referred to as *subsite mapping*. To completely map the binding region of HSA, we determined the number of subsites, located the position of the catalytic amino acids within the subsites and determined the binding energies of each subsite-substrate monomer unit. Quantitative theories of the action pattern of amylase in terms of subsite affinities were proposed independently by Hiromi et al. [14] and Allen and Thoma [15] and later by Suganuma et al. [16]. The procedure described by Allen and Thoma was applied for subsite mapping of HSA and the mutant Y151M since it is suitable for endo-amylases. Recently this method was also used for subsite map calculation of the closely related PPA. The action pattern was determined both on 2-chloro-4-nitrophenyl (CNP)- $\beta$ -glycosides and maltooligosaccharides. Computer modelling on the two different maltooligosaccharide series resulted in the same subsite map for PPA, which verifies that the presence of CNP group at the reducing end of substrates does not influence the apparent binding energies [17]. In addition, there are some subsite maps published in the literature for distantly related amylases, e.g. from *Aspergillus oryzae*, *Bacillus licheniformis*

\*Corresponding authors. Fax: (36)-52 512913.

E-mail addresses: [kandra@tigris.klte.hu](mailto:kandra@tigris.klte.hu) (L. Kandra), [ramasun1@umdnj.edu](mailto:ramasun1@umdnj.edu) (N. Ramasubbu).

**Abbreviations:** HSA, human salivary  $\alpha$ -amylase; HPA, human pancreatic  $\alpha$ -amylase; PPA, porcine pancreatic  $\alpha$ -amylase; BCF, bond cleavage frequency; CNP, 2-chloro-4-nitrophenyl; DP, degree of polymerization; HPLC, high-performance liquid chromatography

(BLA) and *Thermoactinomyces vulgaris*, which clearly show the differences in the binding region of these enzymes [15,18,19].

The active site of human amylases harbors three aromatic residues Trp59, Tyr62 and Tyr151, which provide stacking interactions to the bound glucose moieties. It has already been shown that Tyr151 occurs at subsite (+2) and may influence the size of the leaving group. To study the role of subsite (+2) in recognition of terminal residue of substrate a mutant Y151M was generated in which the tyrosine at position 151 of HSA was replaced by a methionine [20].

Present studies were aimed at evaluating the subsite maps of HSA and Y151M mutant by utilizing as model substrates CNP- $\beta$ -glycosides of maltooligosaccharides with varying degree of polymerization (DP) 3–10. A computer program, which was developed by Gyémánt et al. [17] according to the synopsis of Allen and Thoma [15], was used for subsite mapping of HSA and the Y151M mutant.

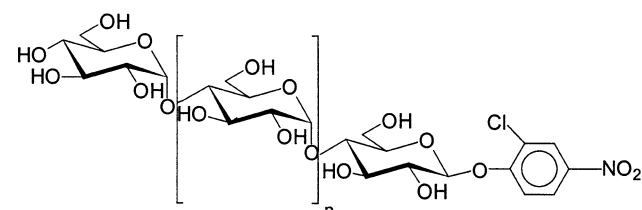
## 2. Materials and methods

### 2.1. Enzymes

$\alpha$ -Amylase (EC 3.2.1.1) from human saliva (Type IXA Sigma) gave a single band on sodium dodecyl sulfate–polyacrylamide gel electrophoresis (SDS–PAGE) and possessed no  $\alpha$ - and  $\beta$ -glycosidase activity. The mutant Y151M enzyme was produced as previously described [20].

The Y151M enzyme was purified by a combination of ion exchange chromatography and size exclusion chromatography (data not shown). The SDS–PAGE and Western blot analyses showed a very intense band of approximate size 55 kDa in the culture medium corresponding to the recombinant enzyme. As with the expression of wild-type enzyme, hexosamines were not detected in the amino acid analysis indicating that the expressed protein was non-glycosylated. Approximately 5 mg of the protein was finally recovered from 1 l culture comparable to the amount recovered for HSA. MALDI-TOF MS (matrix-assisted laser desorption/ionization time-of-flight mass spectrometry) analysis of the mutant showed a molecular mass of 56.22 kDa corresponding to non-glycosylated enzyme.

### 2.2. Substrates



CNP- $\beta$ -maltooligosaccharides DP 3–7 were synthesized from  $\beta$ -cyclodextrin [21]. The longer chain length of CNP-maltooligosaccharides in the range of DP 8–10 was prepared by a chemoenzymatic procedure described earlier by Kandra et al. [22].

Table 1  
Yields of products from the hydrolysis of CNP-maltooligosaccharides by HSA

Substrate	Products (mol%)						
	CNP-G1	CNP-G2	CNP-G3	CNP-G4	CNP-G5	CNP-G6	CNP-G7
CNP-G3	–	–					
CNP-G4	10	85	5				
CNP-G5	2	86	12				
CNP-G6		51	44	5			
CNP-G7		18	50	30	2		
CNP-G8		16	27	41	16		
CNP-G9		17	19	26	30	8	
CNP-G10		17	29	16	11	19	8

### 2.3. Hydrolysis of maltooligosides

Incubations in 25 mM glycerophosphate buffer (pH 7.0) containing 5 mM Ca(OAc)<sub>2</sub> and 50 mM NaCl were carried out at 37°C for 2, 5 and 10 min. The reactions were initiated by the addition of enzyme (final concentration of 1.85 nM HSA and 18.8 nM Y151M) to the solution containing 1.0 mM of substrate. Samples (20  $\mu$ l) were taken at the indicated time intervals and the reaction was stopped by the injection of the samples into the chromatographic column. In these studies we have taken care to exclude the secondary attack on the products by obtaining the product ratios from the early stages of hydrolysis wherein the conversion was always <10%.

Catalytic efficiencies which were calculated from the hydrolysis data measured with CNP-G7 substrate by high-performance liquid chromatography (HPLC) show that Y151M has remarkably decreased affinity ( $k_{\text{cat}}/K_M$ : 106 s<sup>−1</sup> mM<sup>−1</sup>) compared to the catalytic efficiency of HSA ( $k_{\text{cat}}/K_M$ : 2678 s<sup>−1</sup> mM<sup>−1</sup>).

### 2.4. Chromatographic analysis

For HPLC a Hewlett-Packard 1090 Series II liquid chromatograph equipped with a diode array detector, automatic sampler and Chem-Station was used. The samples were separated on Spherisorb ODS2 5  $\mu$ m column (250  $\times$  4.0 mm) with acetonitrile:water (13:87) as the mobile phase and at a flow rate of 1 ml/min at 40°C. The effluent was monitored for CNP-glycosides at 302 nm and the products of the hydrolysis were identified by using relevant standards (Fig. 1).

## 3. Results and discussion

The application of homologous oligomeric substrates is an effective way to explore the nature of the binding site and the process of catalysis for  $\alpha$ -amylases. Although the overall structure and the tertiary folding of the polypeptide chains of different  $\alpha$ -amylases have been determined [23], less is known about the differences in the action of  $\alpha$ -amylases on the homologous maltooligosaccharide series and only a few subsite maps have been evaluated for  $\alpha$ -amylases until now [15,16,18,19,24]. The use of  $\beta$ -CNP-maltooligosaccharides as probes for subsite mapping has been successful in the study of the action pattern and subsite mapping of PPA and BLA (*B. licheniformis*  $\alpha$ -amylase) [17,25], albeit small differences that might be expected from the true subsite map due to perturbation caused by the  $\beta$ -linked chromophore residue. Compared with other substrate series so far reported, for example, maltooligosaccharides [26] or  $\alpha$ -NP-maltooligosaccharides [27], the CNP-maltooligosaccharides, which are  $\beta$ -glycosides, are unique since the  $\beta$ -linkage is stable and is not hydrolyzed by  $\alpha$ -amylases. Therefore, the reducing end products of hydrolysis are always  $\beta$ -glycosides and lead to clear identification of the site of cleavage using UV detection.

### 3.1. Action pattern and cleavage frequencies of HSA on CNP-maltooligosides

A series of CNP-maltooligosaccharides DP 3–10 was used

as substrates for HSA and the products were analyzed using HPLC to determine unambiguously the exact glycosidic linkage being cleaved, as well as the cleavage frequency, an indicator of the binding mode of the corresponding substrate. The chromatographic conditions are given in Section 2. The products containing the CNP moiety were quantified using a diode array detector at 302 nm. The concentrations of glycosidic fragments produced by amylase reaction showed linearity with the reaction time, and the distribution of products was calculated for a given substrate. Table 1 summarizes the product ratios for HSA.

HSA exhibits a unique pattern of action on CNP-malto-oligosaccharides by cleaving CNP-G2 units as the main products; 85%, 86% and 51% from the reducing end of CNP-G4, CNP-G5 and CNP-G6, respectively. As the chain length increases, the maximum frequency of attack shifts toward the non-reducing end of the chain and a more equal distribution between the potential products of longer substrates is observed. Nevertheless, the release of maltotetraose is always dominant; 51%, 50%, 41% and 30% from CNP-G6, CNP-G7, CNP-G8 and CNP-G9, respectively.

The number of subsites in HSA has been reported to be five based on kinetic data measured with modified oligosaccharides [7,8]. In this model, the subsite architecture consists of three glycone and two aglycone subsites. In a later study, Nagamine et al. [28] proposed that there are seven subsites in tandem. Based on crystal structure analysis, it was suggested that the active site of HSA could consist of up to seven subsites [3]. Recently the action pattern of oligosaccharides shorter than heptaose was explained by the five subsite model, while for the interpretation of results from heptaose hydrolysis, additional subsites were invoked [20]. The recent report on the acarbose complexes of HSA and a deletion mutant (lacking residues 306–310 of HSA) shows that the hexasaccharide was bound at the active site of native enzyme while a heptasaccharide was present in a deletion mutant [10]. Present study confirms that the binding region in HSA is longer than five subsites, and strongly suggests the presence of at least seven subsites; four glycone- and three aglycone-binding sites at the reducing end.

### 3.2. Action pattern and cleavage frequencies of Y151M on CNP-maltooligosides

The product distribution for Y151M mutant, on the same oligosaccharide series, was very interesting and markedly different from that of the HSA (Table 2). The moiety CNP-G1 is the major product of hydrolysis when CNP-G3 and CNP-G4 were used as substrates. Thus, hydrolysis of CNP-G3, CNP-G4 and CNP-G5 resulted in 77%, 76% and 34% CNP-G1

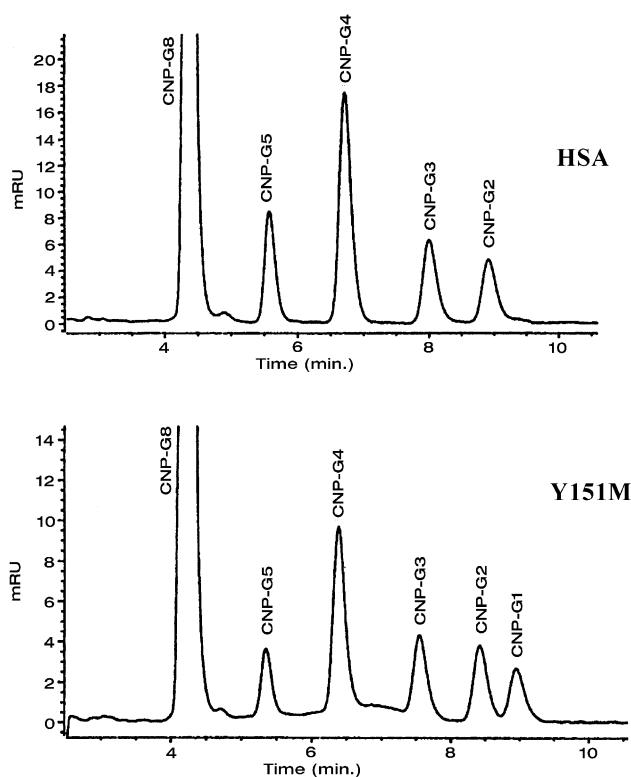


Fig. 1. HPLC chromatogram of CNP-G8 hydrolysis products catalyzed by HSA and Y151M mutant. Injected volume: 20  $\mu$ l.

compared to 0%, 10% and 2% CNP-G1 when HSA was used as a catalyst. There is marked reduction in the amount of CNP-G2 produced in the hydrolysis of CNP-G4 and CNP-G5 catalyzed by HSA (85% and 86% CNP-G2, respectively, vs. 17% and 54%, respectively for Y151M) (Tables 1 and 2). This suggests a favorable interaction between the glucose moiety and subsite (+1), but a less favorable one between the glucose residue and subsite (+2).

The moiety CNP-G1 was significantly released in the hydrolysis of longer oligomers (DP 6–10) as well whereas this monomer glycoside was not recognizable as a product in the hydrolysis of the corresponding substrates by HSA. In this mutant the point of cleavage moved closer to the reducing end by one subsite resulting in a clear shift in the action pattern. This tendency is evident for all of the substrates DP 3–10. These results can be explained by the presence of methionine at subsite (+2) which is not advantageous to the polar glucose residues. This residue may not provide as strong

Table 2  
Yields of products from the hydrolysis of CNP-maltooligosaccharides by Y151M

Substrate	Products (mol%)						
	CNP-G1	CNP-G2	CNP-G3	CNP-G4	CNP-G5	CNP-G6	CNP-G7
CNP-G3	77	23					
CNP-G4	76	17	7				
CNP-G5	34	54	4	8			
CNP-G6	10	63	26	1			
CNP-G7	8	25	33	34			
CNP-G8	10	18	17	38	17		
CNP-G9	8	30	14	18	24	6	
CNP-G10	7	16	25	11	11	15	15

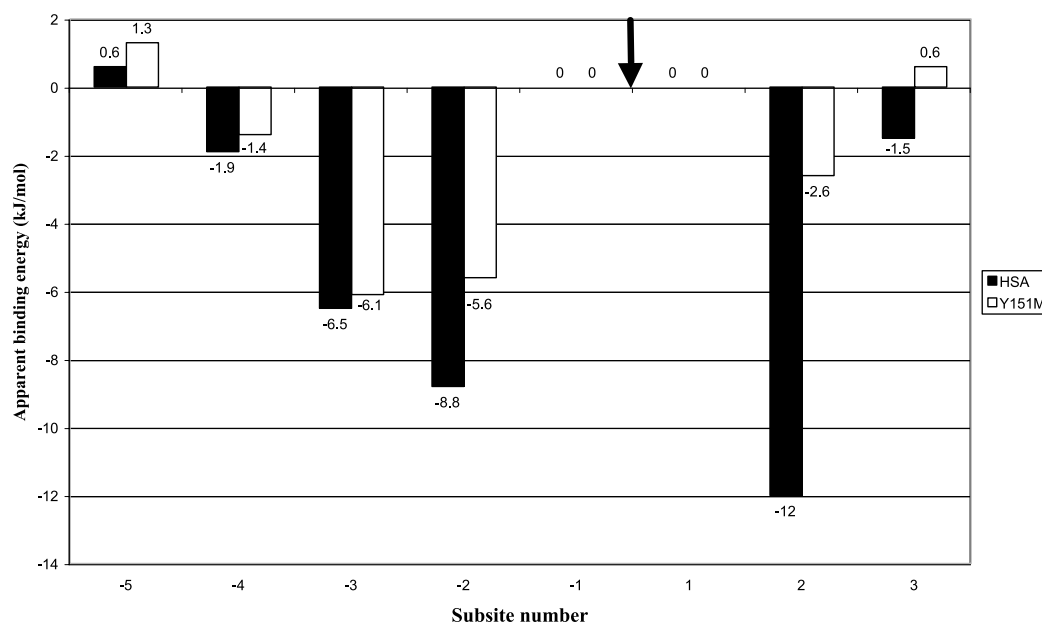


Fig. 2. Subsite maps for HSA (solid bar) and Y151M (open bar). The arrow indicates the scissile bond. The reducing end of maltooligomers is situated at the right hand of the subsite map. Negative energy values indicate binding between the enzyme and aligned glucopyranosyl residues, while positive values indicate repulsion.

a stacking and/or hydrophobic interaction as that of the tyrosine present in the wild-type enzyme.

### 3.3. Subsite mapping of HSA and Y151M

Endo-acting enzymes form more productive binding modes resulting in a complex product pattern. The relative rate of formation of each product is called bond cleavage frequency (BCF), which gives information about the subsite-binding energy. By using BCFs for a series of oligomeric substrates, it is possible to calculate the subsite-binding energy for each subsite on the enzyme-binding region, with the exception of the two subsites adjacent to the catalytic site which are occupied by all productive complexes.

The preferred procedure suggested by Allen and Thoma [13] for subsite map calculation is as follows:

- Establish experimental conditions where secondary reactions (transglycosylation, secondary attack) are insignificant.
- Use end-labelled substrates to determine quantitative BCF for chain lengths that are large enough to span the entire binding region.
- Examine BCSs to estimate the number of subsites and the position of the catalytic site.
- Apply a minimization process to test the differences of measured and calculated BCF data.

Fig. 2 shows the apparent binding energies of subsites for HSA and Y151M.

Subsite map shows that four glycone and three aglycone binding sites are present in HSA. Subsite (+3) has a moderate but significant affinity for the glucose residue (−1.5 kJ/mol) and therefore it is reasonable to consider the presence of the third subsite at the aglycone site. This subsite does not exist in Y151M. To clarify the presence of subsite (+3) further structural and biochemical investigations are necessary. Surprisingly, the calculated binding energy at subsite (+2) (−12.0 kJ/mol) indicates a remarkably good interaction with the bound monomer unit compared with the other subsite ener-

gies. This finding is in good agreement with the three-dimensional structural model of HSA described by Ramasubbu et al. [10]. Fig. 3 shows the three-dimensional structure of the active site of HSA and bound inhibitor at subsite (+2).

Although a decreased binding energy was envisaged for subsite (+2) in Y151M, all of the subsites exhibited a lower affinity for a glucose residue compared to the corresponding subsites of HSA. Such a reduction fits well with cooperative binding of the oligosaccharide ligand. The most remarkable decrease in the calculated binding energies can be found at subsite (+2), −2.6 kJ/mol compared to −12.0 kJ/mol when HSA was used. These findings confirm clearly the role of Tyr151 at subsite (+2) and provide evidence that stacking interactions at the reducing end are important in substrate binding and product distribution in the hydrolysis of oligosaccharides catalyzed by HSA. The methionine at position 151

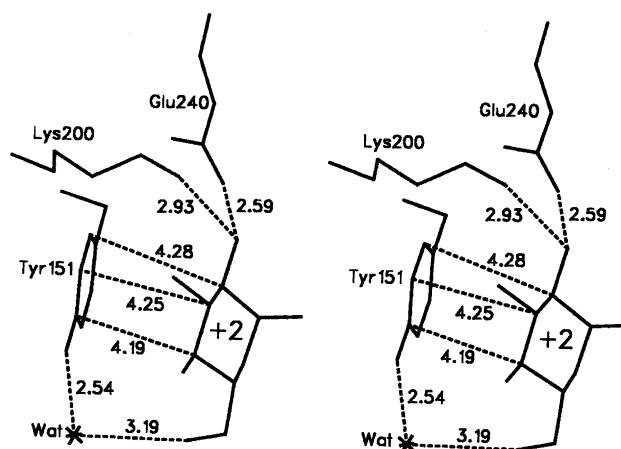


Fig. 3. Stereodiagram of the active center of HSA. The interaction around subsite (+2) in HSA is shown. The residue Tyr151 interacts with subsite glucose through both a stacking interaction and a water molecule. In addition to its interaction with Tyr151, the glucose also has hydrogen-bonding interactions with Lys200 and Glu240.



of HSA would not provide the stacking interaction and the water-mediated hydrogen-bonding interaction provided by the tyrosine residue of HSA. However, the interactions provided by Glu240 and Lys200 would be expected to be present. The considerable reduction in the affinity at subsite (+2) in the mutant suggests that the stacking interaction should be present. The interactions with Lys200 and Glu240 may be secondary which come into play later. Thus, the disappearance of the affinity at subsite (+3) may be dependent upon the absence of several interactions at subsite (+2). The subsite (+3) appears to be more solvent exposed than (+2) as deduced from the crystal structure of the HSA:acarbose complex [10], which also could account for the relatively smaller reduction in the affinity. Nevertheless, the involvement of Tyr151 may be significant in the hydrolysis mechanism of HSA since the productive binding modes for oligosaccharides include the one in which a glucose unit occupies this site. The results of this study show significant differences in the active site architecture of the wild-type and the mutant. The reduction in the affinity may arise due to the side of methionine adopting a conformation, which partially occupies the space which would otherwise be occupied by a glucose.

The tyrosine residue at position 151 of HSA is highly conserved in all mammalian amylases and those which contain a chloride ion near the active site [29]. A tyrosine residue of similar function exists at position 139 in *Tenebrio molitor*  $\alpha$ -amylase, as well [30].

In summary, the tyrosine residue at position 151 of HSA appears to play a major role in the hydrolysis of CNP-substrates by not only affecting the ground state binding but also transition state affinities of the substrates.

**Acknowledgements:** This work was supported by OTKA T032005, and a scholarship from the Hungarian Academy of Sciences (J.R.) and the USPHS Grant DE12585 (N.R.).

## References

- [1] Greenberger, N.J. and Toskes, P.P. (1991) *Harrison's Principles of Internal Medicine*, Vol. 2, 12th edn., 1369 pp., McGraw-Hill, New York.
- [2] Salt, W.B. and Schenker, S. (1976) *Medicine* 55, 269–289.
- [3] Ramasubbu, N., Paloth, V., Luo, Y., Brayer, G.D. and Levine, M.J. (1996) *Acta Crystallogr. D* 52, 435–446.
- [4] Nishide, T., Nakamura, Y., Emi, M., Yamamoto, T., Ogawa, M., Mori, T. and Matsubara, K. (1986) *Gene* 41, 299–304.
- [5] Brayer, G.D., Luo, Y. and Withers, S.G. (1995) *Protein Sci.* 4, 1730–1742.
- [6] Omichi, K. and Ikenaka, T. (1986) *J. Biochem.* 99, 1245–1252.
- [7] Nagamine, Y., Omichi, K. and Ikenaka, T. (1988) *J. Biochem. (Tokyo)* 104, 667–670.
- [8] Omichi, K., Hase, S. and Ikenaka, T. (1992) *J. Biochem. (Tokyo)* 111, 4–7.
- [9] Brayer, G.D., Sidhu, G., Maurus, R., Rydberg, E.H., Braun, C., Wang, Y., Nguyen, N.T., Overall, C.M. and Withers, S.G. (2000) *Biochemistry* 39, 4778–4791.
- [10] Ramasubbu, N., Ragunath, C. and Mishra, P.J. (2003) *J. Mol. Biol.* 325, 1061–1076.
- [11] Phillips, D.C. (1966) *Sci. Am.* 215, 78–90.
- [12] Robyt, J.F. and French, D. (1970) *Arch. Biochem. Biophys.* 138, 662–670.
- [13] Davies, G.J., Wilson, K.S. and Henriessat, B. (1997) *Biochem. J.* 321, 557–559.
- [14] Hiromi, K. (1970) *Biochem. Biophys. Res. Commun.* 40, 1–6.
- [15] Allen, J.D. and Thoma, J.A. (1976) *Biochem. J.* 159, 105–132.
- [16] Suganuma, T., Matsuno, R., Ohnishi, M. and Hiromi, K. (1978) *J. Biochem.* 84, 293–316.
- [17] Gyémánt, G., Hovánszki, G. and Kandra, L. (2002) *Eur. J. Biochem.* 269, 5157–5162.
- [18] Kandra, L., Gyémánt, G., Remenyik, J., Hovánszki, G. and Lipták, A. (2002) *FEBS Lett.* 518, 79–82.
- [19] Shimura, Y., Wang, Q. and Sakano, Y. (1999) *Biosci. Biotech. Biochem.* 63, 2199–2201.
- [20] Mishra, P.J., Ragunath, C. and Ramasubbu, N. (2002) *Biochem. Biophys. Res. Commun.* 292, 468–473.
- [21] Farkas, E., Jánossy, L., Harangi, J., Kandra, L. and Lipták, A. (1997) *Carbohydr. Res.* 303, 407–415.
- [22] Kandra, L., Gyémánt, G., Pál, M., Petró, M., Remenyik, J. and Lipták, A. (2001) *Carbohydr. Res.* 333, 129–136.
- [23] MacGregor, E.A., Janeček, Š. and Svensson, B. (2001) *Biochim. Biophys. Acta* 1546, 1–20.
- [24] Thoma, J.A., Brothers, C. and Spradlin, J. (1971) *Biochemistry* 9, 1768–1775.
- [25] Kandra, L., Gyémánt, G. and Lipták, A. (1997) *Carbohydr. Res.* 298, 237–242.
- [26] Haegele, E.O., Schaich, E., Rauscher, E., Lehmann, P. and Grassl, M. (1981) *J. Chromatogr.* 223, 69–84.
- [27] MacGregor, A.W., Morgan, J.E. and MacGregor, E.A. (1992) *Carbohydr. Res.* 227, 301–313.
- [28] Nagamine, Y., Omichi, K. and Ikenaka, T. (1988) *J. Biochem. (Tokyo)* 104, 409–415.
- [29] D'Amico, S., Gerday, C. and Feller, G. (2000) *Gene* 253, 95–105.
- [30] Strobl, S., Maskos, K., Betz, M., Wiegand, G., Huber, R., Gomis-Rüth, F.X. and Glockshuber, R. (2000) *J. Mol. Biol.* 278, 617–628.